Authors' responses to Reviewers' comments

Manuscript ID: egusphere-2025-494

Title: Unveiling single-particle composition, size, shape, and mixing state of freshly emitted Icelandic dust via electron microscopy analysis

Authors: Agnesh Panta, Konrad Kandler, Kerstin Schepanski, Andres Alastuey, Pavla Dagsson Waldhauserova, Sylvain Dupont, Melanie Eknayan, Cristina González-Flórez, Adolfo González-Romero, Martina Klose, Mara Montag, Xavier Querol, Jesús Yus-Díez, and Carlos Pérez García-Pando

We would like to thank the reviewers for their careful review of the manuscript and for their helpful suggestions and comments. Below we respond to each of their comments, with the reviewers' comments in normal text and our responses in blue and added text in red.

We believe that these changes have addressed the reviewer's comments and welcome any additional suggestions or feedback from the referees and editor.

On behalf of the co-authors,
Agnesh Panta

Anonymous Referee #3, 31 Mar 2025

In this study, Iceland dust was sampled and measured using scanning electron microscopy. Iceland dust is an important source of dust in the Arctic, contributing to e.g. ice nucleating particles and snow albedo. Therefore, detailed knowledge of these dusts is important and useful. This study provides a huge dataset and describes it well…

Thank you for your constructive and detailed feedback. We appreciate your recognition of the importance of the dataset. We have taken your suggestions into account and have revised the manuscript accordingly. Below are our responses to your specific comments.

… I suggest providing some more SEM images showing the most dominant particle type (e.g., medium Al-mix silicate).

We have now included images and elemental mapping of medium Al-mix silicate particles in the supplementary material.

Section 2.3.1 How many seconds did you use for SEM-EDX analysis?

We now add this information in section 2.3.1.

The X-ray signal was collected for each particle for a duration of 15 to 20 seconds (EDAX) and 2 seconds (Oxford), resulting in a total of 40,000 to 100,000 counts. During this time, the beam scanned over the particle's cross-sectional area.

Page 8, line 150: Samples with bubbles in the substrate; What do you mean by "bubbles"?

By "bubbles" we meant surface detects. The following was added in the text:

Areas with surface defects (for example bubbles in the substrate) were excluded from further analysis.

Page 8, lines 152-153: Which SEM images, secondary or backscattered electron, did you use? If both images, did you use both signals for all particles?

This sentence was inaccurate. We used backscatter electron imagery for particle detection. The following was added in the text:

Automated particle segmentation from the background was performed based on the backscatter electron signal.

Page 9, line 201: Did you use Co in this study? Also, F is included in the criteria (Table 3), but did you measure F?

Co was not used. Relative atomic fractions of the elements C, N, O, F, Na, Mg, Al, Si, P, S, Cl, K, Ca, Ti, V, Cr, Mn, Fe, Zn and Pb were recorded. Note that the given method was not applied to quantify the percentage of C, N, and O due to their high uncertainty and substrate contributions. The following text was added:

The information on the chemistry of each particle consisting of the major elements F, Na, Mg, Al, Si, P, S, Cl, K, Ca, Ti, V, Cr, Mn, Fe, Zn and Pb is derived from EDX and given as normalized atomic percentages. As the substrate is composed of carbon, information on the elements C is discarded while quantifying the particle composition. Owing to the high error, O and N were not considered.

Page 10, line 218 (Section 3.1.1) I suggest showing SEM images of medium Al mixed silicate with elemental mapping images if possible. This particle type is the most abundant and has complex compositions. Therefore, a SEM image and elemental mapping images will help to understand the particles. This study provides few SEM images, i.e., no SEM image in the main text and some SEM images of minor types are shown in the supplementary figures without

further discussion. As this study uses SEM and discusses the particle morphology, more particle images and discussion will be useful.

We have now included elemental mapping of medium Al-mix silicate (MAS) particles in the supplementary material. The following text was added:

For illustration, images and elemental mappings of the MAS particles are given in the electronic supplement (S8 and S9). The glassy structure becomes nicely visible by the river line fractures and the smooth surfaces. In some cases, a pumice structure is recognizable. While small variations in composition are detected, in general this group is homogeneous with respect to composition.

Page 13 lines 274-275. I do not see "ring" in Fig. S4. Please indicate it clearly.

The text has been updated as it was based on an earlier iteration of the presented work referring to another image.

Page 14 Figure 4. Here and in other figures, it is difficult to distinguish the colors within many different particle types. I have no good idea how to distinguish them, but I had a hard time reading it.

We agree that distinguishing between many different particle types based on color can be challenging. We tried to color-code by major geochemical groups: oxides/hydroxides (red tones), feldspar minerals (green tones), salts (blue tones).

In the revised version, we've combined the following groups for the sake of simplifying the display.

- Complex silicate (moderat Al-low alkali), Complex silicate (high Al), Al-rich clay mineral, Other silicate and Ca-rich silicate/Ca-Si mixtures —> **‘Complex silicates’**

- Sea-salt/silicate mixture, Aged sea-salt/silicate mixture, Sodium sulfate/silicate mixture, Sulfate/silicate mixture, Complex mixture —> **‘Mixtures’**

Page 16 lines 319-320. “Fe is either embedded in the lattice structure of the particle itself or present as small Fe”: A SEM image and an elemental mapping image will help with the Fe distribution. I suggest adding them.

We now provide an elemental mapping with Fe distribution in the supplement section S9.

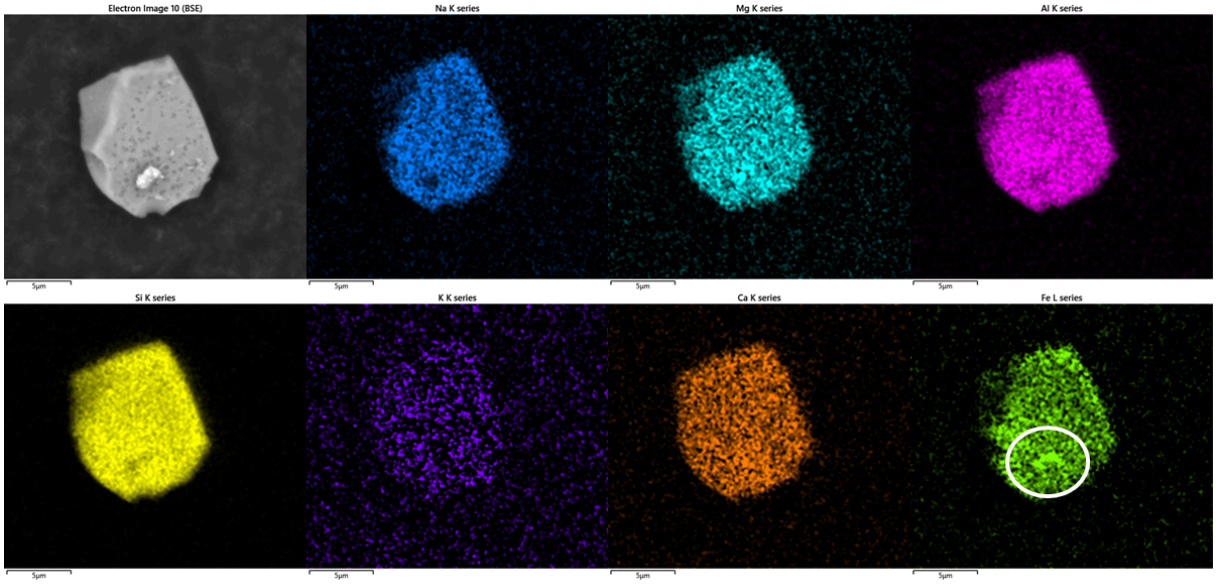

SEM image and corresponding energy dispersive X-ray spectroscopy (EDX) elemental maps of Sodium (Na), Magnesium (Mg), Aluminum (Al), Silicon (Si), Potassium (K), Calcium (Ca), and Iron (Fe) on representative “MAS” particle. Increased brightness indicates more of the element. The white circles emphasize the Fe-rich inclusions.

Supplementally Figures S9 and S10. There is no description of the figures in the main text. Especially Fig. S9 shows interesting features of the particle morphology, but no discussion. There is also no identification of the particle types in Fig. S9. In Fig. S10, although they are useful, there are no SEM images of the most dominant particle type (medium Al-mix silicate). The examples are of minor particle types. In addition, these particles are too large in Figs. S9 and S10 and are not typical of the size range. I suggest showing more typical particle sizes and mineral types in the main text. A low magnification SEM image with many particles would also be interesting to see.

We now add examples images of low-magnification electron micrographs of dust collected by the flat-plate deposition sampler are shown in section S7 Figure S4 of the supplement, giving an impression of the diversity of the dust grains.

Anonymous Referee #4, 02 Apr 2025

This study investigated the Iceland dust, which is important in understanding the source of dust in Arctic. The mineralogical composition, morphology and size distribution were analyzed with ccSEM/EDX. The data set is important and useful for future studies. Overall, this study is well designed and the paper is well written. I think is paper is worth publishing on ACP, and I have a few minor comments to help improve it.

Thank you for your positive feedback and thoughtful suggestions. We appreciate your recognition of the value of the dataset and the overall quality of the paper. We have addressed the comments and suggestions below to improve clarity and the completeness of our study.

General comment:

Could you comment how EDX settings affect penetration depth and affect the results, since you might not get the elemental composition of large particles.

We have added the following discussion in the supplement S2.

In our analysis, we used a lower acceleration voltage of 12.5 kV, which reduces the interaction volume and helps minimize the effects of particle morphology on quantification. This approach has been shown to improve accuracy, particularly for larger particles, by limiting the penetration depth of X-rays (Kandler et al., 2018). While it is true that the penetration depth of a few micrometer might pose a problem for large particles, if they exhibit a strong core-shell structure or other systematic inhomogeneities, in this case it can be expected that the effect is minor. On one hand, the beam is scanned during the analysis over all of the particle cross section, averaging out local effects. On the other hand, the mappings (now in the supplement S9) show a homogeneous horizontal elemental distribution for the dominating particle class, which can therefore be expected to be vertically homogeneous as well (glassy matter). Also, the crystalline compounds are not expected to exhibit a strong vertical inhomogeneity; therefore in this study we can expect that the composition we measure is representative for the total particle volume.

Minor comments:

Line 75-76: it is unclear to me what is “mode of occurrence of Fe”

The term “mode of occurrence of Fe” has been used in prior studies of the same project such as Gonzalez-Romero et al. (2023,2024). The terminology was used due to its general use in prior chemical studies of Fe metal ore minerals where the differentiation between the presence of Fe in different species and/or mineral habitats is crucial.

Line 105 and table 2: mention the full name for the sampling sites when they first appear.
Done

Figure 1: it will be good to explain the relationship between each sub figure.
We now provide figure labels and explain the relationship. The following has been added:

Figure 1. (a) Basemap of Iceland showing the hotspot region of Jökulsá á Fjöllum with dotted points. The yellow star indicates the main experimental site "DYS", and the purple dots mark the locations of deposition samplers in the outflow regions. (b) Zoom-in of the hotspot region showing the samplers "HRS" and "VFS" located northeast of the main site. (c) Zoom-in showing the samplers "SRS" and "MRS" located southwest of the main site.

Table 3: this table is very difficult to follow. I suggest using flow chart.
We decided to show the entire table in SI in a flow chart.

Line 230: How do you identify these are volcanic glass? Could you add figure and explain a little bit more?

X-Ray diffraction (XRD) was used to quantify the mineral phases present and is described in detail in a companion paper González-Romero et al. (2024). Briefly, we refer to this paper here for further details. XRD coupled with the Rietveld method, has been increasingly used as a fast and reliable method to evaluate the content of the crystalline and amorphous phases in inorganic materials (Rietveld, 1969; Cheary and Coelho, 1992; Young, 1993; TOPAS, 2018). Quantification of mixtures via the Rietveld method is generally restricted to crystalline phases for which structures are well known. However, the addition of a known amount of an internal standard material allows the quantification of any amorphous (non-crystalline) material in the mixture that has not been included in the model, in our case, volcanic glass or amorphous alteration products like allophane, imogolite, and silica (De la Torre et al., 2001; Madsen et al., 2001; Scarlett and Madsen, 2006; Machiels et al., 2010; Ibañez et al., 2013). Sample preparation for quantitative mineralogical analysis consisted of preliminary dry grinding of the samples in an agate mortar, mixed with a known amount (10 %–20 %) of CaF2 powder (Merck), as an internal standard to allow the determination of amorphous contents, and finally dry ground again to reduce the grain size distribution and homogenise the mixture. The analysis was carried out by a Bruker D8 A25 Advance powder X-ray diffractometer equipped with a LynxEye 1D position sensitive detector, monochromatic Cu Kα radiation (Å) operating at 40 kV and 40 mA. The diffractograms were recorded by scanning from 4 to 120° of 2θ with a step size of 0.015° and a counting time of 1 s per step maintaining the sample in rotation (15 min−1). The mineral identification was performed by searches and comparisons of the patterns from the International Centre for Diffraction Database (ICDD, PDF-2) using DIFFRAC.EVA software package (Bruker AXS). The quantitative analysis of the mineral phases was carried out by Rietveld full-pattern analyses performed with the TOPAS 5 software (Bruker AXS), which uses least-square procedures to minimise the differences between the observed and calculated diffractograms. The abundances of the crystalline and amorphous phases were normalised to 100 wt % (weight percentage). The quality of the fitting was evaluated by visually comparing the observed and calculated diffractograms to achieve a realistic model and checking the residual factors (RB, Rwp, Rexp) and goodness of fit (GOF) calculated by the TOPAS model (Rietveld, 1969; Toby, 2006).

We have modified this part which now reads:

Furthermore, X-ray diffraction (XRD) analysis was performed on the surface sediments (González Romero et al., 2024b). The XRD analysis revealed that a significant component (79 ± 11 wt %) of the sediment consists of an amorphous phase, most probably volcanic glass and its nano-sized weathering product (hydrated amorphous Si-bearing).

Figure 6: the text and legend are too small and very difficult to read.

We have now updated the figure.

Figure 7 (a): where is the shaded area?

This was a mistake. The caption has been updated. It now reads:

Size-resolved particle AR. The bar range represents the range between 0.1 and 0.9 quantiles with dot being the median and the bins are color coded by the number of data points within each bin.

Line 365-366: The Sulfate episodes show significant difference for different locations. Please add some discussion about the differences.
In this section, we only presented the result. We have discussed the differences in lines 471-481 in the revised text.

Kandler, K., Schneiders, K., Ebert, M., Hartmann, M., Weinbruch, S., Prass, M., and Pöhlker, C.: Composition and mixing state of atmospheric aerosols determined by electron microscopy: method development and application to aged Saharan dust deposition in the Caribbean boundary layer, Atmospheric Chemistry and Physics, 18, 13 429–13 455, https://doi.org/10.5194/acp-18-13429-2018, 2018.

González-Romero, A., González-Florez, C., Panta, A., Yus-Díez, J., Reche, C., Córdoba, P., Moreno, N., Alastuey, A., Kandler, K., Klose, M., Baldo, C., Clark, R.N., Shi, Z.B., Querol, X., Pérez García-Pando, C.: Variability in grain size, mineralogy, and mode of occurence of Fe in surface sediments of preferential dust-source inland drainage basins: The case of the Lower Drâa Valley, S Morocco. Atmos. Chem. Phys., 23, 15815–15834, https://doi.org/10.5194/acp-23-15815-2023, 2023.

González-Romero, A., González-Flórez, C., Panta, A., Yus-Díez, J., Córdoba, P., Alastuey, A., Moreno, N., Kandler, K., Klose, M., et al, 2024. Probing Iceland's dust-emitting sediments: particle size distribution, mineralogy, cohesion, Fe mode of occurrence, and reflectance spectra

signatures. Atmos. Chem. Phys., 24, 6883-6910, https://doi.org/10.5194/acp-24-6883-2024, 2024.

González-Romero, A., González-Flórez, C., Panta, A., Yus-Díez, J., Córdoba, P., Alastuey, A., Moreno, N., Hernández-Chiriboga, M., Kandler, K., Klose, M. and Clark, R.N., 2024. Characterization of the particle size distribution, mineralogy, and Fe mode of occurrence of dust-emitting sediments from the Mojave Desert, California, USA. Atmos. Chem. Phys., 24, 9155-9176, https://doi.org/10.5194/acp-24-9155-2024, 2024.

Rietveld, H. M.: A profile refinement method for nuclear and magnetic structures, J. Appl. Crystallogr., 2, 65–71, 1969.

Cheary, R. W. and Coelho, A.: A fundamental parameters approach to X-ray line profile fitting, J. Appl. Crystallogr., 25, 109–121, 1992.

Young, R. A.: The Rietveld method. International Union of Crystallography, Oxford University Press, UK, https://doi.org/10.1017/S0885715600019497, 1993.

TOPAS: TOPAS and TOPAS-Academic: an optimization program integrating computer algebra and crystallographic objects written in C++, J. Appl. Cryst., 51, 210–218, 2018.

De la Torre, A. G., Bruque, S., and Aranda, M. A. G.: Rietveld quantitative amorphous content analysis, J. Appl. Crystallogr., 34, 196–202, 2001.

Madsen, I. C., Scarlett, N. V. Y., Cranswick, L. M. D., and Lwin, T.: Outcomes of the international union of crystallography commission on powder diffraction round robin on quantitative phase analysis: Samples 1a to 1h, J. Appl. Crystallogr., 34, 409–426, 2001.

Scarlett, N. and Madsen, I.: Quantification of phases with partial or no known crystal structures, Powder Diffr., 21, 278–284, 2006.

Machiels, L., Mertens, G., and Elsen, J.: Rietveld Refinement strategy for Quantitative Phase analysis of Partially Amorphous zeolitized tuffaceous, Geol. Belg., 13, 183–196, 2010.

Ibáñez, J., Font, O., Moreno, N., Elvira, J. J., Alvarez, S., and Querol, X.: Quantitative Rietveld analysis of the crystalline and amorphous phases in coal fly ashes, Fuel, 105, 314–317, 2013.

Toby, B. H.: R factors in Rietveld analysis: How good is good enough?, Powder Diffr., 21, 67–70, https://doi.org/10.1154/1.2179804, 2006.

Anonymous Referee #1, 18 Apr 2025

This study investigates the composition, size, shape, and mixing state of freshly emitted Icelandic dust particles collected in the Dyngjusandur desert using scanning electron microscopy/energy dispersive X-ray spectroscopy (ccSEM/EDX). Analyzing over 190,000 particles, the results reveal that Medium-Al mixed silicates (MAS), likely volcanic glass, are the most abundant particle type. The study also identifies sulfate particles indicative of volcanic influence, as well as iron- and titanium-rich particles. Icelandic dust exhibits a size-dependent increase in aspect ratio, unlike Moroccan dust. The findings highlight key differences between Icelandic and Moroccan dust, including higher iron and titanium content and a lack of potassium. This research contributes valuable data for improving models simulating the role of high-latitude dust in the Earth system.

We appreciate your recognition of the importance of the dataset. We have taken your suggestions into account and have revised the manuscript accordingly. Below are our responses to your specific comments.

Line 23-26：The original text briefly mentions the importance of mixing state for optical properties and chemical processes but doesn't provide a detailed conceptual framework or examples of how mixing structures influence aerosol behavior. The authors should add references here about the regional aerosol mixing regime framework, highlighting the diversity and heterogeneity of ambient particles. E.g.: Li et al. (2016). 112, 1330–1349. https://doi.org/10.1016/j.jclepro.2015.04.050

We have revised the introduction to better contextualize the significance of aerosol mixing state by expanding the conceptual discussion and including an additional reference as suggested. The revised sentence now reads:

Moreover, the distribution of the compounds in and among the particles (i.e., internal or external mixing) is another important factor to consider. For example, the optical properties of aerosols, such as light absorption and scattering, are strongly dependent on their mixing state (Lindqvist et al., 2014; Nousiainen and Kandler, 2015). In addition, chemical transformation processes, such as heterogeneous reactions and secondary aerosol formation, are also considerably affected by whether particles are internally or externally mixed (Ito and Feng, 2010). The mixing state can vary substantially depending on the regional aerosol regime and emission sources, reflecting the diverse and heterogeneous nature of ambient particulate matter (Li et al., 2016). Understanding these mixing structures is essential for assessing aerosol impacts on climate and air quality.

Line 33-34：There are contradictory statements like "HLD sources associated with glaciers will be increasingly active in the future as temperatures increase and glaciers retreat". However, the increased precipitation due to climate change can reduce dust emission from glacier areas. The impact of glaciation on dust particle emissions under climate warming needs to be further verified.

We have revised the text to reflect this complexity and to acknowledge that the net effect of climate change on HLD emissions remains an active area of research requiring further verification. The revised sentence now reads:

Some studies suggest that HLD sources may become more active in the future as glaciers retreat and expose new sediments (Bullard et al., 2016, Meinander et al. 2022). While factors such as changes in precipitation and vegetation cover could counteract this effect by stabilizing dust source areas (Aryal et al. 2023), field observations from Iceland demonstrate that precipitation has limited influence on dust suspension from glacial outwash plains. Dust storms have been observed during high precipitation periods and even with low winds, with dust plumes occurring within hours after rainfall (Dagsson-Waldhauserova et al., 2014). Further work is needed to understand the net effect on HLD emissions due to climate change.

Line 57-68: The introduction highlights the lack of in-situ studies but doesn't critically assess the existing literature's limitations. A more pointed discussion of why previous studies are insufficient (e.g., limited sampling, inadequate analytical techniques, lack of source characterization) would set the stage more effectively.

We have expanded the relevant section of the introduction to more clearly articulate the limitations of existing in-situ studies. The revised section now reads:

Information on the physico-chemical differences across dust sources is essential for dust modeling and understanding its climate impact. The mineralogical composition of dust can differ greatly between regions because of geological and climatic influences (Claquin et al., 1999; Journet et al., 2014). However, many Earth models generally assume a globally uniform dust composition, due to the lack of comprehensive global data on the parent soil. Only a few models consider variations in dust mineralogy (Perlwitz et al., 2015; Gonçalves Ageitos et al., 2023; Song et al., 2024) by utilizing global soil type atlases and extrapolating from a small set of analyses. In situ studies, which could provide more accurate data, are often limited by several challenges. For one, source areas are difficult to study due to the remote and harsh nature of source regions, as well as the technical difficulties in sampling during high dust events. Instruments used for measuring dust in these conditions are often prone to saturation or damage, further complicating data collection. Moreover, the large size range, spanning from few microns to hundreds of microns, of mineral dust particles adds another layer of complexity. Field measurements often struggle to capture the larger supermicron particles, which constitute a significant fraction of the total mass. Additionally, different sampling methods based on properties such as optical, inertial, or electrical characteristics often yield data that are difficult to compare, as these methods depend on particle composition, size, and shape. Without parallel measurements of physico-chemical properties, the data from different techniques can be difficult to reconcile (Hinds, 1999). These issues underscore the need for more robust, in-situ studies that can provide high-resolution data on particle composition, size distribution, and source characterization to improve the accuracy of dust-climate interaction models.

Lines 105-113: The description of the sampling sites lacks crucial detail regarding the surface characteristics. Specifying the types of soil, vegetation cover at each site is essential to understand the representativeness of the collected dust.
We have added descriptions of the sampling site.

The main site (DYS) was located in a terminal lake connected to a nearby glacier (N 64° 54' 55", W 16° 46' 35", 710 m a.s.l.; see Fig. 1). The area is topographically mostly flat and is devoid of vegetation or other obstacles. It has however melt water channels due to the glacier discharge causing glacio-fluvial sediment to be frequently replenished with finer particles on top, that are prone to dust emission under favourable conditions (González-Romero et al., 2024b; Dupont et al., 2024). The main site (DYS) was heavily instrumented with several ground-based monitoring devices for meteorological and airborne dust measurements. In addition to the main measurement site, dust deposition samplers were deployed throughout the region to study the spatial distribution and composition of dust. These auxiliary sites are labeled MRS, SRS, HRS, and VFS (see Fig. 1). MRS and SRS are located near DYS, while HRS and VFS are positioned further downwind, with VFS situated on a hilltop. MRS, SRS, and HRS have surface characteristics similar to the main site and are part of the Jökulsá á Fjöllum river basin. VFS is located approximately 60 meters above the riverbed and is well-positioned to monitor airborne dust leaving the riverbed source.

Lines 121-122: Temporal resolution mismatch: FPS has longer integration times (8-48 h) compared to FWI (minutes to 1 h). This temporal mismatch can be problematic if the aerosol composition or concentration changes significantly during FPS sampling.

The variation in integration times arises from the fundamental difference in operating principles between the samplers. The Flat Plate Samplers (FPS) operate passively, with significantly lower effective collection velocities, whereas the FWI is an active system with much higher ones. Applying the same short sampling duration to passive samplers would result in insufficient particle loading for analysis, while extending the sampling time of active samplers could lead to filter overloading and loss of resolution.
To clarify this point, we have added the following text to the manuscript:

The differences in sampling durations reflect the distinct operational modes of the samplers. Passive samplers (i.e. FPS), require longer integration times (8–48 h) to accumulate sufficient aerosol loading due to their low collection velocities. In contrast, active samplers (i.e. FWI) can operate over much shorter time frames (minutes to 1 h), as their high effective collection velocities ensure adequate particle loading. Matching the durations across all systems would either result in under-loading of passive samples or overloading of active filters.

Except during the sulfate intrusion period, the composition remains relatively constant (see Fig. S2 and S3). Therefore, we divided the data into two categories: 'sulfate episodes' and 'excluding sulfate episodes'. This aggregation was done primarily because collection efficiency by size is less relevant to the fractional contribution of each mineral type within a given size range. By integrating both techniques, we improve the statistical robustness for each size category, as more particles are analyzed.

Lines 236-242: The discussion of pyroxene/amphibole-like particles lacks quantitative analysis. The manuscript does not provide the percentage of these particles relative to the total aerosol population.

The quantitative discussion on the particle composition including pyroxene/amphibole-like particles is presented in section "*3.2 Relative abundances of various types of particles"* of the manuscipt.

Table 4: Aspect Ratio (AR) distributions for various particle types are presented without explicitly linking AR to the broader mineral groups of Table 3, thus undermining group classifications and relationships.

We have added the discussion regarding the major particle type and their aspect ratio distributions. The following text has been added:

The variability in AR across different particle types is generally limited, except for ammonium-sulfate-like particles, which show a broader range of AR values—particularly in the coarse and super-coarse size fractions. This increased variability likely reflects the more irregular and diverse morphologies of these particles at larger sizes. Overall, AR tends to increase with particle size across all particle types, suggesting that size has a stronger influence on particle morphology than mineralogical composition. This size-dependent trend implies that larger particles, regardless of mineral type, are more likely to exhibit elongated or irregular shapes. The AR distribution is slightly narrower in the fine size range, with a median of 1.37, whereas the coarse and super-coarse ranges show broader distributions, with medians of 1.46 and 1.53, respectively. This broader AR spread at larger sizes is mainly driven by the high variability observed in MAS particles. Despite these differences, the overall shape of the AR distribution is relatively consistent with that observed in Morocco.

Lines 267-275: The original text briefly mentions the formation of sulfate particles from SO_2 but doesn't elaborate on the chemical modification of dust particles through heterogeneous reactions. The authors should provide references in this section that detail the use of electron microscopy to analyze sulfate modification of dust minerals. E.g.: Li et al., (2014). 119(2), 1044–1059. https://doi.org/10.1002/2013JD021003

We now provide a reference that used SEM to analyze sulfate modification of mineral dust. As most of the sulfate identified does not contain any Na, Mg, K or Ca, we assume that it is mainly from gas-to-particle conversion.

Furthermore, some mineral dust particles (e.g., calcite) can transform into other particle types through heterogeneous reactions with SO_2 (Li et al., 2014). Most of the sulfate observed falls into the group of Ammonium sulfate-like particles due to the lack of the common cations like Na, Mg, K or Ca, which is consistent with its formation by gas-to-particle conversion from the volcanic plume (Boulon et al., 2011).

Lindqvist, H., Jokinen, O., Kandler, K., Scheuvens, D., and Nousiainen, T.: Single scattering by realistic, inhomogeneous mineral dust particles with stereogrammetric shapes, Atmospheric Chemistry and Physics, 14, 143–157, https://doi.org/10.5194/acp-14-143-2014, 2014.

Nousiainen, T. and Kandler, K.: Light scattering by atmospheric mineral dust particles, pp. 3–52, Springer Berlin Heidelberg, Berlin, Heidelberg, https://doi.org/10.1007/978-3-642-37985-7_1, 2015.

Ito, A. and Feng, Y.: Role of dust alkalinity in acid mobilization of iron, Atmospheric Chemistry and Physics, 10, 9237–9250, https://doi.org/10.5194/acp-10-9237-2010, 2010.

Li, W., Shao, L., Zhang, D., Ro, C.-U., Hu, M., Bi, X., Geng, H., Matsuki, A., Niu, H., and Chen, J.: A review of single aerosol particle studies in the atmosphere of East Asia: morphology, mixing state, source, and heterogeneous reactions, Journal of Cleaner Production, 112, 1330–1349, https://doi.org/10.1016/j.jclepro.2015.04.050, preventing Smog Crises, 2016.

Bullard, J. E., Baddock, M., Bradwell, T., Crusius, J., Darlington, E., Gaiero, D., Gassó, S., Gisladottir, G., Hodgkins, R., McCulloch, R., McKenna-Neuman, C., Mockford, T., Stewart, H., and Thorsteinsson, T.: High-latitude dust in the Earth system, Reviews of Geophysics, 54, 447–485, https://doi.org/10.1002/2016RG000518, 2016.

Meinander, O., Dagsson-Waldhauserova, P., Amosov, P., Aseyeva, E., Atkins, C., Baklanov, A., et al. (2022). Newly identified climatically and environmentally significant high-latitude dust sources. Atmos. Chem. Phys. 22, 11889–11930. doi:10.5194/acp-22-11889-2022

Aryal, Y. and Evans, S.: Dust emission response to precipitation and temperature anomalies under different climatic conditions, Science of The Total Environment, 874, 162 335, https://doi.org/10.1016/j.scitotenv.2023.162335, 2023.

Claquin, T., Schulz, M., and Balkanski, Y. J.: Modeling the mineralogy of atmospheric dust sources, J. Geophys. Res.-Atmos., 104, 22243–22256, https://doi.org/10.1029/1999JD900416, 1999.

Journet, E., Balkanski, Y., and Harrison, S. P.: A new data set of soil mineralogy for dust-cycle modeling, Atmos. Chem. Phys., 14, 3801–3816, https://doi.org/10.5194/acp-14-3801-2014, 2014.

Perlwitz, J. P., Pérez García-Pando, C., and Miller, R. L.: Predicting the mineral composition of dust aerosols – Part 2: Model evaluation and identification of key processes with observations, Atmos. Chem. Phys., 15, 11629–11652, https://doi.org/10.5194/acp-15-11629-2015, 2015

Gonçalves Ageitos, M., Obiso, V., Miller, R. L., Jorba, O., Klose, M., Dawson, M., Balkanski, Y., Perlwitz, J., Basart, S., Di Tomaso, E., Escribano, J., Macchia, F., Montané, G., Mahowald, N.

M., Green, R. O., Thompson, D. R., and Pérez García-Pando, C.: Modeling dust mineralogical composition: sensitivity to soil mineralogy atlases and their expected climate impacts, Atmospheric Chemistry and Physics, 23, 8623–8657, https://doi.org/10.5194/acp-23-8623-2023, 2023.

Song, Q., Ginoux, P., Gonçalves Ageitos, M., Miller, R. L., Obiso, V., and Pérez García-Pando, C.: Modeling impacts of dust mineralogy on fast climate response, Atmospheric Chemistry and Physics, 24, 7421–7446, https://doi.org/10.5194/acp-24-7421-2024, 2024.

Hinds, W.: Aerosol Technology : Properties, Behavior, and Measurement of Airborne Particles, Wiley Interscience, 1999.

González-Romero, A., González-Flórez, C., Panta, A., Yus-Díez, J., Córdoba, P., Alastuey, A., Moreno, N., Kandler, K., Klose, M., Clark, R. N., Ehlmann, B. L., Greenberger, R. N., Keebler, A. M., Brodrick, P., Green, R. O., Querol, X., and Pérez García-Pando, C.: Prob ing Iceland's dust-emitting sediments: particle size distribution, mineralogy, cohesion, Fe mode of occurrence, and reflectance spectra signatures, Atmospheric Chemistry and Physics, 24, 6883–6910, https://doi.org/10.5194/acp-24-6883-2024, 2024

Dupont, S., Klose, M., Irvine, M. R., González-Flórez, C., Alastuey, A., Bonnefond, J.-M., Dagsson-Waldhauserova, P., Gonzalez-Romero, A., Hussein, T., Lamaud, E., Meyer, H., Panta, A., Querol, X., Schepanski, K., Vergara Palacio, S., Wieser, A., Yus-Díez, J., Kandler, K., and Pérez García-Pando, C.: Impact of Dust Source Patchiness on the Existence of a Constant Dust Flux Layer During Aeolian Erosion Events, Journal of Geophysical Research: Atmospheres, 129, e2023JD040 657, https://doi.org/10.1029/2023JD040657, 2024.

Dagsson-Waldhauserova, P., Arnalds, O., Olafsson, H., Skrabalova, L., Sigurdardottir, G.M., Branis, M., Hladil, J., Skala, R., Navratil, T., Chadimova, L., von Lowis of Menar, S., Thorsteinsson, Th., Carlsen, H.K., and Jonsdottir I., 2014. Physical properties of suspended dust during moist and low wind conditions in Iceland. Icelandic Agricultural Sciences 27: 25 – 39

Li, W., Shao, L., Shi, Z., Chen, J., Yang, L., Yuan, Q., Yan, C., Zhang, X., Wang, Y., Sun, J., Zhang, Y., Shen, X., Wang, Z., and Wang, W.: Mixing state and hygroscopicity of dust and haze particles before leaving Asian continent, Journal of Geophysical Research: Atmospheres, 119, 1044–1059, https://doi.org/10.1002/2013JD021003, 2014.

J. Boulon, K. Sellegri, M. Hervo, & P. Laj, Observations of nucleation of new particles in a volcanic plume, Proc. Natl. Acad. Sci. U.S.A. 108 (30) 12223-12226, https://doi.org/10.1073/pnas.1104923108 (2011).